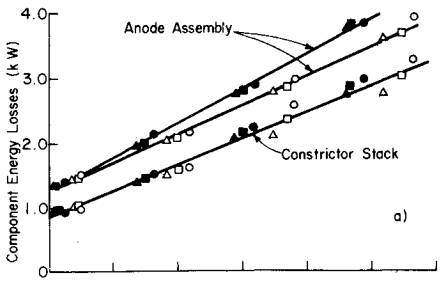

Fig. 1a Constrictor stack and anode assembly losses vs power input.

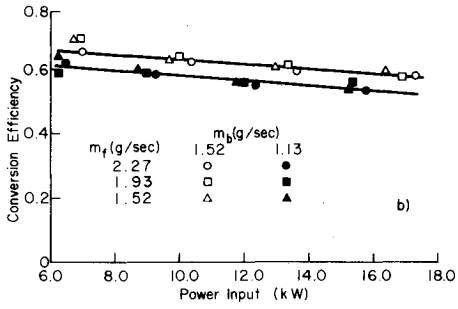

Fig. 1b Energy conversion efficiencies vs power input for current levels of 126, 171, 214, and 258 amp.

mm diam and of length 27.4 mm while the corresponding dimensions for the anode are 12.7 mm and 11.1 mm. Cremers et al.[1] discuss the choice of materials and the anode configuration.

The energy losses to the constrictor stack and the anode assembly are shown in Fig. 1a for film flow rates ($\dot{m}_f$) of 2.27, 1.93, and 1.52 g/sec, base flow rates ($\dot{m}_b$) of 1.52 and 1.13 g/sec, and for current levels of 126, 171, 214, and 258 amp. The obvious grouping of the data points arises from variation in the arc voltage drop when the arc current is maintained constant but the argon flow rates are changed. The losses to the constrictor stack show little dependence on the film and base flow rates except as those flow rates affect the electric field, and thereby the arc voltage drop, in the constrictor channel. Such an effect of the base flow is expected, while that of the film flow shows that the film does exert a squeezing effect on the arc in the anode throat, can cause a slight increase in density upstream, and thus affects the electric field and the heat transfer coefficient. This is not a large effect; in fact, a 15% increase in $\dot{m}_f$ with constant $\dot{m}_b$ will cause about a 3% change in the over-all arc voltage drop.

The energy transferred to the anode by the electrons, which constitute almost all of the arc current and which condense on the anode surface, is the dominant energy input to the anode assembly (in contrast to the constrictor stack losses that depend on the flow and electric fields as well as the arc current, i.e., the rate at which the energy is dissipated, within the constrictor channel). An increase in the base flow rate causes an increase in the arc voltage drop; thus, for a given power input, the arc current and the anode assembly losses are smaller. This effect accounts for the dependence of the anode assembly losses on the base flow rate.

A decrease in the film flow rate lessens the protection provided by the film and the anode surface temperature will increase. This leads to the more diffuse arc attachment explained in Ref. 1. Visual observations of the incandescent portion of the anode surface confirm that, as either the film flow is decreased while maintaining constant current and base flow or as the current is increased at constant argon flow rates, the arc attachment area increased. The data also show that the energy loss at the anode decreased for smaller $\dot{m}_f$ and constant current and $\dot{m}_b$. A smaller anode fall voltage accounts for this.

The visual observations also showed that the tangential injection of the base flow did not drive the arc attachment point circumferentially over the anode surface in the ranges of flow rates considered. Increasing the base flow rate to the maximum obtainable with the equipment available (2.27 g/sec) and decreasing the film flow rate to the point where rapid ablation of the anode occurred (1.0 g/sec) did not cause the arc attachment to move. Radial injection of the base flow and tangential injection of the film should alleviate this difficulty.

The energy conversion efficiency is defined as the energy output to a calorimeter divided by power input and is shown versus power input in Fig. 1b. A clear dependence on the base flow rate exists while the film flow rate has only a small effect. The efficiencies are comparable with, or at best only slightly higher than, those of similar generators with purely water-cooled anodes. Variation of the cooling water flow to the anode has only small effects in the range considered (0.064–0.079 kg/sec).

References

[1] Cremers, C. J., Shiver, W. D., and Birkebak, R. C., "Film-Cooling of a Plasma Generator Anode," *AIAA Journal*, Vol. 6, No. 9, Sept. 1968, pp. 1774–1776.

[2] Davis, L. B., "A Study of Film-Cooling on the Anode of an Arc Plasma Generator," M.S. thesis, May 1970, Univ. of Kentucky, Lexington, Ky.

Roughness Effects on Heat Transfer in the Supersonic Region of a Conical Nozzle

MEYER RESHOTKO*
NASA Lewis Research Center, Cleveland, Ohio

As part of the study on the effects of roughness in conical nozzles heat-transfer results were obtained in the supersonic region up to Mach 4.4. This paper will concentrate on the region between Mach 1.7 and 4.4 where the acceleration drops off from the high values in the vicinity of the throat to the low values near the nozzle exit. This is an area of particular interest to those who use rough surfaces to simulate the effects of ablation that take place upon re-entry. A material such as graphite after undergoing ablation will have a surface texture similar to those discussed in this paper.

A number of experiments have been recently conducted (Ref. 1-6) on the effects of flow acceleration with and without surface roughness on heat transfer. In these cases the favorable pressure gradient was obtained by passing the working fluid through a converging-diverging nozzle. Flow acceleration represented by velocity and pressure gradient are shown in Fig. 1 as a function of axial distance from the throat. Main interest was directed at the region of highly accelerated flow which is upstream of and in the vicinity of the throat. It was in this region that there was an appreciable difference between the experimental heat-transfer results and the existing correlations. The results are given in detail in Refs. 4–6 and summarily in Fig. 2 for the representative case of $M = 0.48$. It can be seen (Fig. 2) that for a smooth wall there are two distinct regimes of heat-transfer rate that

Received April 8, 1971.

* Aerospace Research Engineer. Associate Member AIAA.

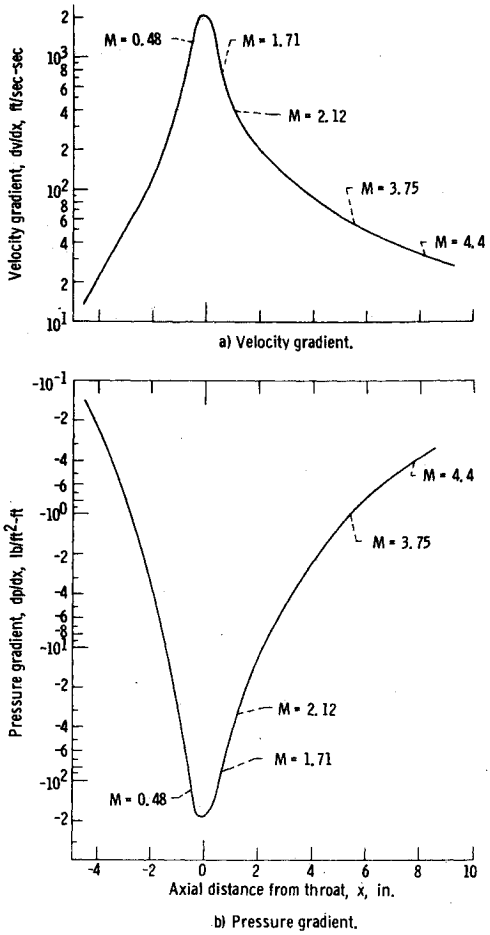

Fig. 1 Velocity and pressure gradient as a function of axial distance from the throat.

are both less than that of the conventional turbulent correlation. The high Reynolds number regime represents turbulent heat transfer for accelerated flows and the low Reynolds number regime suggests a laminarization phenomenon. If wall roughness is introduced with values up to 325 μ in. rms, the results of Fig. 2 show that: 1) detransition from the turbulent mode of heat transfer takes place at a lower Reynolds number than that for a smooth wall. 2) The effect on heat transfer in the laminarization region is negligible. An additional result from Ref. 5 is: 3) heat transfer in the turbulent regime does not seem to be noticeably affected until the roughness height exceeds a given height which corresponds to the approximated sublayer height.

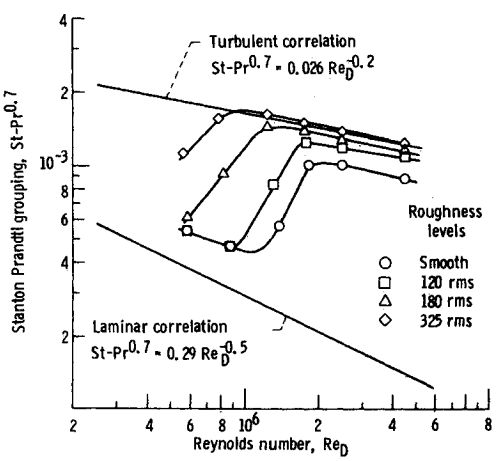

Fig. 2 Heat transfer for smooth and rough surfaces in highly accelerated flow at M = 0.48.

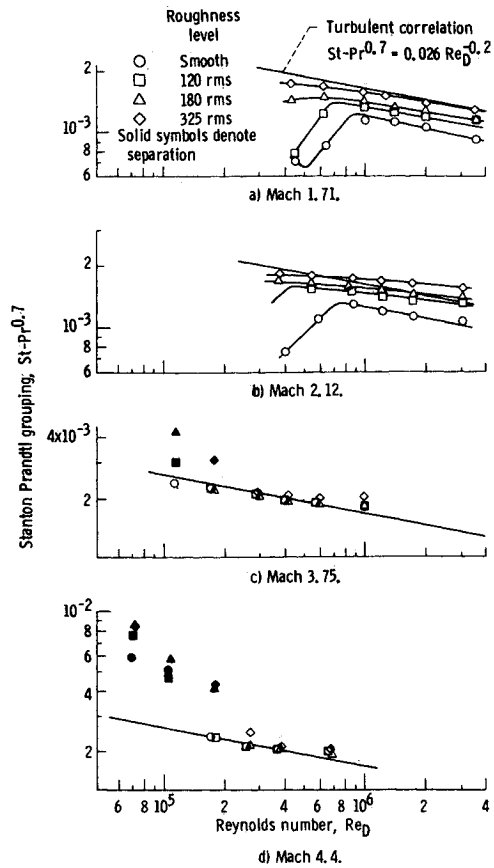

Fig. 3 Experimental heat transfer for various degrees of roughness in supersonic flow: a) Mach 1.71. b) Mach 2.12. c) Mach 3.75. d) Mach 4.4.

Information concerning apparatus, measurements, method of roughening, and data reduction are covered in Refs. 1 and 5. A 30° half-angle of convergence by 15° half-angle of divergence nozzle was roughened by a sandblasting technique to roughness levels up to 325 micro in. rms. Air at a stagnation temperature of 970°R was used as the working fluid. The stagnation pressure was varied from 30–300 psia yielding almost an order of magnitude range in Reynolds number at each station.

Heat-transfer data with roughness as a parameter is presented in Fig. 3 for the supersonic region of Mach 1.7–4.4. Heat transfer in the form of a Stanton-Prandtl number grouping, St-$Pr^{0.7}$, is plotted with respect to Reynolds number with surface roughness as a parameter. The diameter is chosen as the reference dimension in the Reynolds number since it is approximately proportional to the boundary-layer thickness which, of course, would be a more appropriate dimension if it were known. Therefore, it must be remembered that two points at the same Reynolds number based on diameter, but at different stations, will not necessarily have the same heat transfer.

At Mach 1.71 one can see the effects of decreasing acceleration on heat transfer in comparison to the high acceleration results portrayed in Fig. 2. There is only one point that has undergone laminarization and only two examples of detransition from the turbulent mode of heat transfer. At Mach 2.12 there is no laminarization, but some evidence of detransition. There is also an over-all increase in the heat-transfer parameter for all surface conditions with the smooth wall heat-transfer parameter approaching the turbulent correlation. The heat-transfer results at Mach 3.75 (Fig. 3c) are unlike anything seen so far in the current study. There is no evidence of either detransition or laminarization. At the four highest Reynolds numbers surface roughness does not affect the heat-transfer parameter. All the heat-transfer

values fall on or near the turbulent correlation line. At the two lower Reynolds numbers there are some data points for the rougher walls that are noticeably above the correlation line. At Mach 4.4 (Fig. 3d), the highest Mach number reached in this study, the heat-transfer values either fall on the correlation line or at the lower Reynolds numbers appreciably above it. In Ref. 2, among others, it is shown that the boundary layer thins down upstream of the throat, reaches a minimum near the throat, and then proceeds to thicken downstream of the throat. At Mach 3.75 and 4.4, the boundary layer is much thicker than it would be at the throat and consequently the same holds true for the sublayer height. In the vicinity of the throat the higher values of surface roughness protrude through the sublayer and cause a heat transfer increase (Ref. 5). However, in the high Reynolds number region of the two high Mach number cases all the roughness heights are contained within the thick sublayer and consequently roughness does not affect the heat transfer. Those data points indicated by the solid symbols represent flow separation which was determined by the fluctuations in the static pressure. Other than indicating that separation has taken place, the data points represented by the solid symbols have no meaning in Figs. 3c and d.

In order to get an over-all picture of roughness effects on heat transfer in the supersonic region of a conical nozzle let us again look at Fig. 1. The scope of this Note is the region where the acceleration decreases and the pressure gradient becomes less favorable. Mach 3.75 and 4.4 are in a region where the favorable pressure gradient is very small, less than $\frac{1}{2}$ of 1% of maximum. One would expect the heat transfer at these Mach numbers to behave as they would under a zero pressure gradient. The results shown in Fig. 3 bear this out for those points not undergoing separation. The heat-transfer parameters compare very favorably with the turbulent correlation. There is no laminarization or detransition. The roughness values used in this Note do not affect the heat transfer which is probably due to a thick boundary layer resulting from the negligible pressure gradient.

At Mach 1.71 and 2.12 the acceleration and favorable pressure gradient are relatively high, but they are less than their respective maxima and dropping off very fast. The resulting heat transfer has some of the characteristics of the maximum acceleration (Fig. 2) but to a lesser degree. Although roughness still affects the heat transfer because the boundary layer has not yet become very thick, there is less evidence of detransition and hardly any of laminarization, two major characteristics of highly accelerated flow.

References

[1] Boldman, D. R., Neumann, H. E., and Schmidt, J. F., "Heat Transfer in 30° and 60° Half-Angle of Convergence Nozzles with Various Diameter Uncooled Pipe Inlets," TN D-4177, 1967, NASA.

[2] Graham, R. W. and Boldman, D. R., "The Use of Energy Thickness in Prediction of Throat Heat-Transfer in Rocket Nozzles," TN D-5356, 1969, NASA.

[3] Back, L. H., Massier, P. F., and Cuffel, R. F., "Flow Phenomena and Convection Heat Transfer in a Concial Supersonic Nozzle," *Journal of Spacecraft and Rockets*, Vol. 4, No. 8, Aug. 1967, pp. 1040–1047.

[4] Boldman, D. R., Schmidt, J. F., and Gallagher, A. K., "Laminarization of a Turbulent Boundary Layer as Observed from Heat-Transfer and Boundary-Layer Measurements in Conical Nozzles," TN D-4788, 1968, NASA.

[5] Reshotko, M., Boldman, D. R., and Ehlers, R. C., "Heat-Transfer in a 60° Half-Angle of Convergence Nozzle with Various Degrees of Roughness," TN D-5887, 1970, NASA.

[6] Reshotko, M., Boldman, D. R., and Ehlers, R. C., "Effects of Roughness on Heat Transfer in Conical Nozzles," *Augmentation of Convective Heat and Mass Transfer*, ASME, 1970.

Spin Rate Behavior of ISIS-I

F. R. VIGNERON,* D. HARRISON,† AND G. BOWER‡
Communications Research Center, Ottawa, Canada

Nomenclature

$\mathbf{B}$ = Earth's magnetic field vector
$\bar{B}^2$ = time average over an orbit of the square of the component of the Earth's field resolved on a normal to the satellite spin axis
C = moment of inertia, 7.7312×10^9 g-cm^2
p = eddy current damping resistivity constant
s = spin rate
t = time
T = torque
$\mathbf{V}$ = satellite orbital velocity

THE spin rate behavior of ionospheric sounding satellites with long flexible antennas in crossed dipole configuration has been of continuing interest since the launch of Alouette I in 1962.[1] Flight data from Alouette I and Explorer XX show a slow decay of spin rate, which may be attributed mainly to a 'solar motoring torque' resulting from an interaction between the solar pressure field and the flexible antennas.[2–4] This Note discusses spin rate data obtained from the ISIS-I[5] ionospheric sounding satellite launched in 1969, in the light of solar motoring and other possible despin torque mechanisms.

Measured spin rate data of ISIS-I taken from date of launch to July of 1970 are shown in Fig. 1. In general, the characteristic slow decay of spin rate is observed. Discontinuities in spin rate on days 91, 97, 243 and so forth, result from the operation of the ISIS control system.[6] Also shown on Fig. 1 are the percent sun variation and the measured variation of solar aspect angle (the angle between the spin axis and the sun line). The measured right ascension and codeclination of the spin axis are presented in Fig. 2.

The data between attitude maneuvers of days 100 and 243 of 1969 shows a period of high despin in the neighborhood of day 160 (Fig. 1). A fifth-order polynomial least-squares fit is found to provide an acceptable analytical model over the 143 day interval, as shown in Fig. 3. A torque history con-

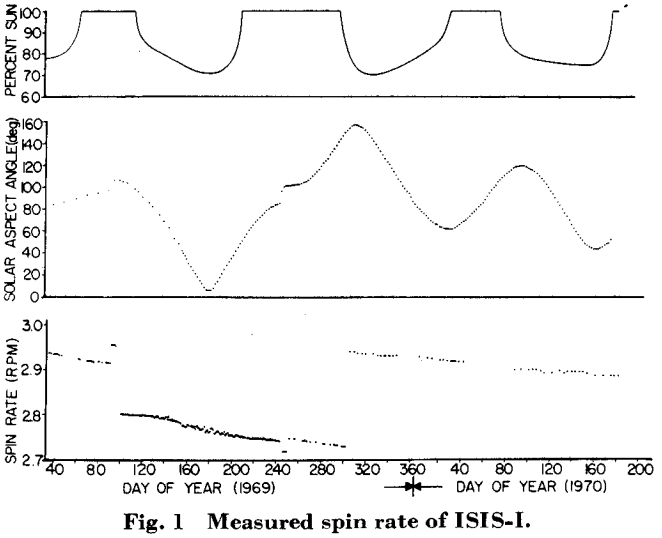

Fig. 1 Measured spin rate of ISIS-I.

Received February 24, 1971; revision received May 27, 1971. Index category: Spacecraft Attitude Dynamics and Control.

* Research Scientist. Member AIAA.
† Engineer, Space Mechanics Section.
‡ Electronics Technician, Space Mechanics Section.